We are IntechOpen, the world's leading publisher of Open Access books Built by scientists, for scientists

4,800
Open access books available

122,000
International authors and editors

135M
Downloads

Our authors are among the

154
Countries delivered to

TOP 1%
most cited scientists

12.2%
Contributors from top 500 universities

CLARIVATE ANALYTICS BOOK CITATION INDEX INDEXED

WEB OF SCIENCE™

Selection of our books indexed in the Book Citation Index in Web of Science™ Core Collection (BKCI)

Interested in publishing with us?
Contact book.department@intechopen.com

Numbers displayed above are based on latest data collected.
For more information visit www.intechopen.com

4

Analysis of the *K* Satellite Lines in X-Ray Emission Spectra

M. Torres Deluigi and J. Díaz-Luque
Universidad Nacional de San Luis
Argentina

1. Introduction

When electromagnetic radiation or particles interact with matter, and they are energetic enough, they can produce the ejection of electrons from the atoms, so the latter become ionized. The ionization can be achieved either by irradiation with a conventional x-ray tube (which emits the characteristic x-radiation of the anode material and a copious amount of white radiation over a wide wavelength range), or by impact with electrons (or heavier particles) accelerated in a suitable gun.

The emission of x-ray from an excited ion arises from a single electron transition between the states with final and initial vacancies. This is primarily because of the strong electric dipole selection rule, which remains dominant for all save the shortest wavelength x-rays (i.e. $\lambda \leq 100$ pm). This selection rule requires that the quantum number for the orbital angular momentum shall change by only one unit during the transition, i.e.:

$$\Delta l = \pm 1 \tag{1}$$

The probability that an incident photon (or particle) causes the ejection of a particular electron is proportional to the square of the integral:

$$\int \Psi_i P \Psi_f \tag{2}$$

where P is the transition operator, and Ψ_i , Ψ_f are the wave functions for the initial and final states of the system, respectively (Urch, 1985). An approach to this integral can be obtained by replacing the wave functions Ψ_i and Ψ_f by those of the orbitals directly involved in the transition, and considering that all the other orbitals are not affected. So, Ψ_i should be replaced by the orbital φ_i from which the electron was ejected, and Ψ_f should be replaced by the orbital φ_f from which comes the electron that will fill the initial vacancy. Furthermore, if we consider the electric dipole (er) approximation for P, the integral (2) can be replaced by the following:

$$\int \varphi_i (er) \varphi_f \tag{3}$$

If the electron is removed from an inner orbital (or core orbital), then the resulting ion may relax in two ways:

a. either by emitting an x-ray that results from an electronic transfer from an external orbital ionization energy E_j to an inner orbital ionization energy E_i. The energy of the emitted photon, which characterizes the levels involved, will be:

$$h\nu = E_i - E_j \tag{4}$$

b. or ejecting an Auger electron, which will leave a doubly ionized atom with vacancies in orbitals φ_j and φ_k. The energy of the Auger electron will be approximately:

$$E = E_i - E_j - E_{k'} \tag{5}$$

where $E_{k'}$ is the ionization energy for an electron from an orbital k in an atom with an atomic number which is one greater than the atom under consideration.

2. Characteristic x-rays

The x-ray spectrum emitted by the sample is produced by simple electronic transitions, which allow more straightforward interpretations than those of the Auger spectra. When only considering the electric dipole vector of radiation, x-ray emission from an excited ion is governed by simple rules of selection ($\Delta l = \pm 1$ and $\Delta j = 0, \pm 1$). The probability of relaxation via the magnetic vector or the electric quadrupole is less, by at least two orders of magnitude, than that for relaxation involving dipolar emission (Urch, 1979). The selection rules give rise to a series of x-rays which are called 'diagram lines' because the basic electronic transitions can be easily represented on a single line diagram as shown in Fig. 1.

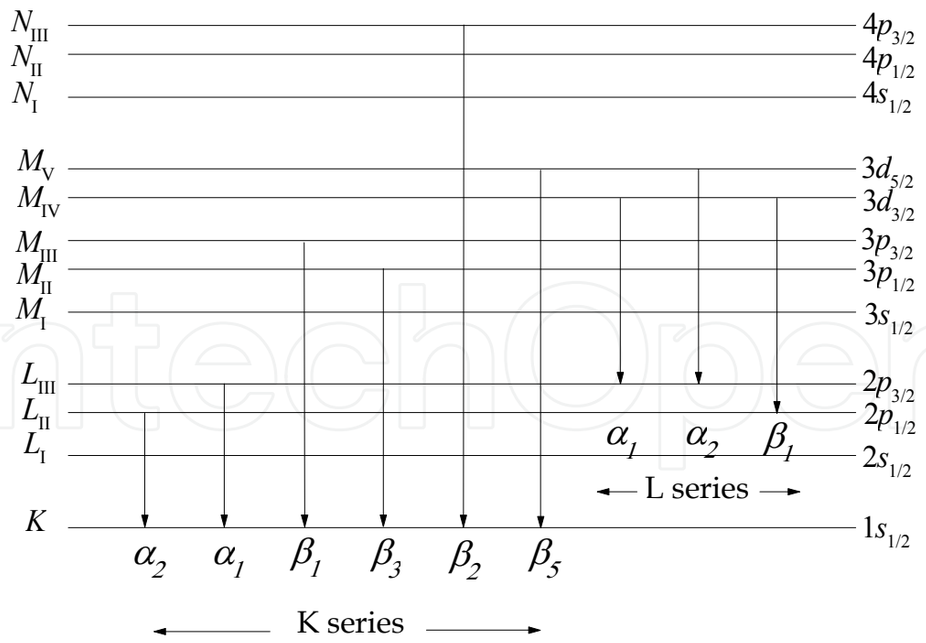

Fig. 1. Emission diagram of the x-ray lines of an atom. Lines *K* and *L*.

When a *K*-shell electron is removed producing a $1s^{-1}$ vacancy, it can be replaced by a *p* electron from layers *L*, *M* or *N* (see Fig. 1). If the transition occurs from a state $2p_{3/2}$, it emits

a characteristic x-ray $K\alpha_1$; however, if the replacement is from $2p_{1/2}$, it emits a photon $K\alpha_2$. On the other hand, if the transition occurs from layers *M* or *N*, i.e., $3p \rightarrow 1s^{-1}$, $3d \rightarrow 1s^{-1}$ or $4p \rightarrow 1s^{-1}$, it produces a characteristic photon emission of the *K*β spectrum.

The transition rules may also be extended to the lines originating from molecular orbitals of the valence band. The emitted spectrum will then have information on the contribution of atomic orbitals to molecular orbitals.

The intensity *I* of x-rays emitted is given by the Einstein equation, which has the following form (Eyring, 1944):

$$I = cte \cdot \nu^3 \cdot \left[\int \Psi_i \, P \, \Psi_f \right]^2 \tag{6}$$

where Ψ_i and Ψ_f are complete wavefunctions for the initial and final states, before and after the x-ray emission respectively, and P is the transition operator. In the one electron approximation, it is assumed that only the orbitals directly involved in the transition need to be considered. The effects of relaxation and electronic reorganization in other molecular orbitals attendant upon the creation of the initial vacancy, and also in the final state after the x-ray has been emitted, are ignored. Since other orbitals are assumed unaffected, this approach is also called the 'frozen orbital' approximation.

Thus, as in the case of equation (2), Ψ_i will be replaced by the atomic orbital for the initial vacancy φ_i, and Ψ_f by the (atomic or molecular) orbital with the final vacancy. When Ψ_f is to be replaced by a molecular orbital (ψ_f), the simplest form will be the Linear Combination of Atomic Orbitals (LCAO):

$$\psi_f = \sum a_{f,\lambda} \varphi_\lambda \tag{7}$$

where $a_{f,\lambda}$ is a coefficient describing the contribution of atomic orbitals φ_λ of the atom λ to the molecular orbital ψ_f.

These molecular orbitals, which are solutions of the Schrödinger equation, can be calculated in various degrees of approximation using tools of quantum mechanics. The energies of the molecular orbitals (occupied and unoccupied) and its composition in terms of electronic populations of the constituent atomic orbitals can be obtained by theoretical models.

There are several computational methods that calculate the molecular orbitals; some of them are, in order of increasing sophistication: the extended Huckel method, the method of Fenske-Hall and the methods Xα (Cotton and Wilkinson, 2008). Among them, the one that shows greater agreement with the experimental spectra is the Discrete Variational Xα (DV-*X*α), that was shown for sulfur compounds by Mogi (Mogi et al., 1993), Uda (Uda et al., 1993) and Kawai (Kawai, 1993), and for manganese and chromium by Mukoyama (Mukoyama et al., 1986). This method first calculates the atomic orbitals φ_λ using the approximation of Hartree-Fock-Slater (HFS) for each constituent atom. The atomic wave functions obtained numerically are used as base functions to construct the molecular wave functions. The elements of the secular matrix are calculated using the DV method and this matrix is then diagonalized to obtain eigenvalues and eigenfunctions of the molecular orbital (Adachi et al., 1978).

The detail with which an x-ray peak will reflect the molecular orbital structure of a molecule or solid will be, apart from experimental considerations, a function of the line widths of the

constituent peaks. In addition, the line widths will be determined by the lifetimes of the initial and final states of the ion between which the transition occurs.

3. Satellite lines

An x-ray emission line (or diagram line) resulting from a transition between two levels in the energy-level diagram is frequently accompanied by satellites lines (or non-diagram lines), i.e., x-ray lines whose energies do not correspond to the difference of two energy levels of the same atom. The term 'satellite' means weak lines close to the strong parent (or diagram) lines. Particle induced x-ray emission (PIXE) spectra, electron probe microanalysis (EPMA) x-ray spectra, or x-ray fluorescence (XRF) spectra of materials exhibit intensity modifications of satellite lines from one compound to another. The satellite lines are classified into three groups by its origin: 1) multivacancy satellites; 2) charge-transfer satellites for late transition-metal compounds; 3) molecular-orbital splitting satellites (Kawai, 1993).

3.1 Multivacancy satellites

The $K\alpha$ lines usually show high-energy satellite lines, corresponding to the existence of a specific number (i) of 'spectator' vacancies in the layer L, which affect the subsequent transitions. These peaks can be identified generally as $K\alpha L^i$, and they appear on the side of higher energies of the main line $K\alpha_{1,2}$. This kind of satellite lines are called multivacancy satellites lines, and among them we find the double ionization caused by $K\alpha L^1$ (or simply $K\alpha L$): when 1s and 2p vacancies are created simultaneously, the 2p vacancy has a relatively long life-time compared to that of the 1s vacancy. Thus, the inner vacancy de-excites in presence of a 'spectator hole' which produces a change in the electrostatic potential, leading to shifts in the energy levels, affecting as a result the energy of the photon emitted (Fig. 2). In this chapter we will study the satellite lines produced by double and triple vacancies in the $K\alpha$ spectrum of aluminium.

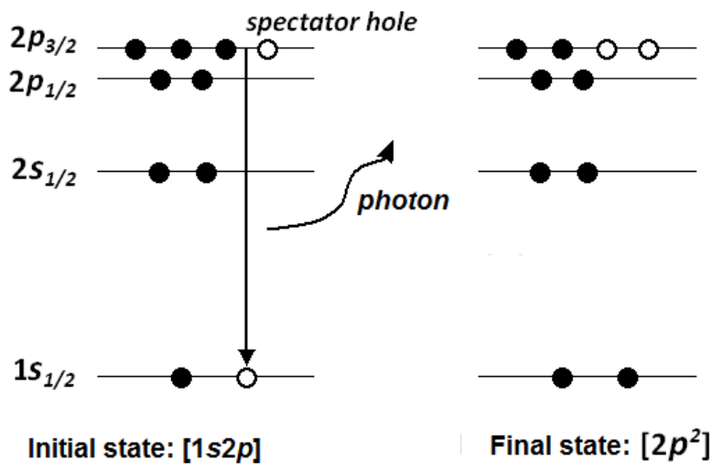

Fig. 2. Emission of a satellite line by double ionization (orbitals with vacancies are enclosed in brackets).

The high energy satellite lines have been intensively studied since the 1930s to the 1940s, beginning with the detailed works of Parrat (Parratt, 1936; 1959; Randall and Parratt, 1940).
In the case of the $K\alpha$ emission line, the high energy satellites are usually labeled as $K\alpha_{3,4}$. The high energy satellite resulting from the de-excitation in presence of two outer vacancies is referred as $K\alpha_{5,6}$ and exhibits a very weak amplitude. The energy separation distance between the satellite band and the $K\alpha$ line ranges from about 10 eV up to about 40 eV for atomic numbers $12 < Z < 30$. Aberg (Aberg, 1927) presents an extensive set of values for the relative intensity of the satellite, which decreases from about 30 % for Z = 10 to 0.5 % at Z = 30.
The KL^n satellite intensity has a close relation to the electronegativity of the neighboring atoms of the x-ray emitting atom, as shown by Watson et al. (Watson et al., 1977), Uda et al. and Endo et al. (Uda et al., 1979; Endo et al., 1980). This is because the KL^n satellite is stronger for ionic compounds than it is for covalent compounds: The valence electrons are delocalized for covalent compounds, thus the perturbation due to the creation of the core-hole is small for said compounds. Consequently, the multielectron ionization probability is small for covalent compounds. On the other hand, for ionic compounds, the valence electrons are localized, thus the perturbation due to the core-hole creation is large. Therefore, the satellites are strong for ionic compounds. Hence, the satellite intensity is a measure of valence electron delocalization, so we can determine the covalence/ionicity of compounds or delocalization/localization of valence electrons by measuring the multivacancy satellites of x-ray emission spectra (Kawai, 1993).
The de-excitation of an *L* or *M* level in presence of outer holes may also lead to the presence of high energy satellites associated with *L* or *M* x-ray peaks. The additional outer vacancies may result from Coster-Kronig transitions or shake-off mechanisms. The Coster-Kronig transitions result from an Auger process between sub-shells of the same shell. For instance, the hole created on the L_1 sub-shell may be filled by an electron originating from the L_2 or L_3 subshell. According to the selection rules, these transitions are not radiative and the excess of energy L_1-L_2 or L_1-L_3 is dissipated by the emission of an Auger electron from the *M* or *N* levels. The transition rate of non-radiative Coster-Kronig transitions f_{ij}, where i and j are two subshells within the same energy level, is not permitted for all elements (Rémond, 2002).
The double excitation threshold is the value of energy needed to cause double vacancies in the atoms, so the probability to observe satellite lines $K\alpha$ is zero for incident energies below this value. Therefore, the formation of double vacancy is only possible for values equal or superior to the threshold, and the satellite spectra are variable according to the energy that excites the sample. The effects of variation of the $K\alpha$ satellite spectrum depending on the excitation energy can be seen, for example, in the work of Oura et al. (Oura et al., 2003). These authors bombarded NaF samples and measured the intensity of the lines KL^1 in the F, from the double excitation threshold to saturation. Fig. 3 shows the different spectra obtained with the different energies for the incident photons (indicated on the right vertical axis). The double excitation threshold is 706.7 eV for F, energy value around which their measures began, and for which the satellite lines are not even seen.
The multivacancy satellites in x-ray emission spectra are lines of importance in PIXE spectra: When heavy ions (such as Ar^{5+}, N^+ or O^{2+}, with an energy of several tens of MeV) bombard the sample material to ionize the core electron, these satellites turn out to be stronger than the diagram lines.

In Fig. 4 it is shown the proton-excited spectrum, which consists of the normal $K\alpha_{1,2}$ peak and $K\alpha_{3,4}$ satellite group. The $K\alpha_{5,6}$ group and other satellites have lower intensity and, in consequence, were not measured with proton excitation. In the case of nitrogen-ion excitation, the spectrum is radically different: A relatively weak line appears at the position of the normal $K\alpha_{1,2}$. The five peaks on the high-energy side of the $K\alpha_{1,2}$ line are $K\alpha$ satellites lines from atoms with one through five vacancies in the *L* shell (Knudson, 1971). We can also see the increasing intensity of the lines of the spectrum $K\beta$, and the emergence of new satellite lines in this region.

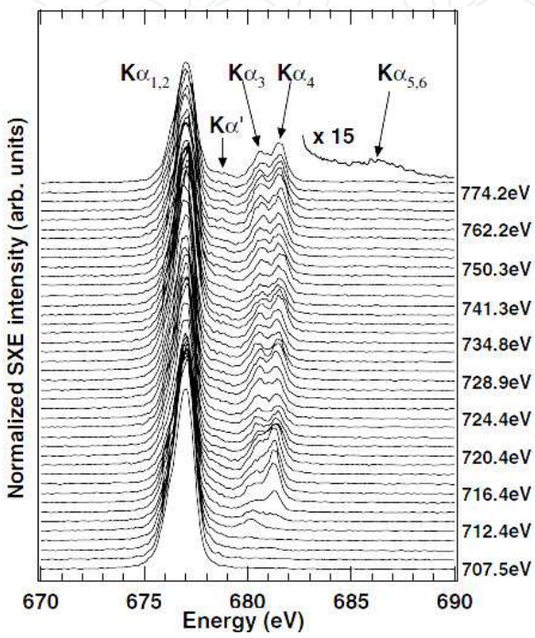

Fig. 3. Spectral variation of the F $K\alpha$ emission for NaF. Typical energies of the exciting photons are indicated beside each spectrum (Oura et al., 2003).

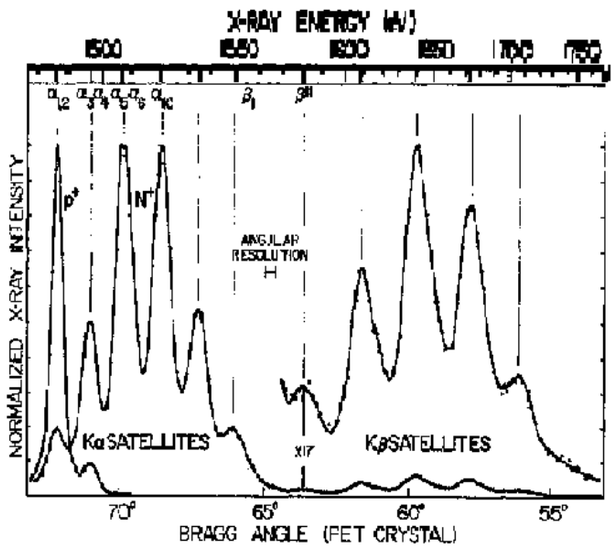

Fig. 4. Al $K\alpha$ x-ray spectra excited by impact of 5 MeV protons and nitrogen ions on Al metal, (Knudson, 1971).

3.1.1 Double and triple vacancy satellite lines in Al *K*α

At higher energies than $K\alpha_{1,2}$ we find the satellite spectrum KL^1 consisting of lines (in increasing order of energy value) $K\alpha'$, $K\alpha_3$ and $K\alpha_4$. At even higher energies we can also observe satellite lines by triple ionization (KL^2), called $K\alpha_5$ and $K\alpha_6$. In this section, we present the results of our measurements for these lines of multiple vacancies for pure aluminum and alumina (Al_2O_3), with XRF and EPMA. The KL^2 satellites are the highest order of ionization obtained by bombarding with photons and electrons, and they have even lower intensities than KL^1. All these lines can be seen in Fig. 5, which presents the experimental intensities of the Al $K\alpha$ spectrum on a logarithmic scale to facilitate its appreciation.

The spectra obtained with XRF and EPMA were fitted with the software Peakfit. This software employs the method of least squares to approximate peaks of the Voigt Gaussian / Lorentzian type to the lines, by setting residuals. Comparing Fig. 6 and Fig. 7 we see that there is an increase in the intensities of the satellite lines by double and triple vacancy with respect to the main lines, when measured with EPMA.

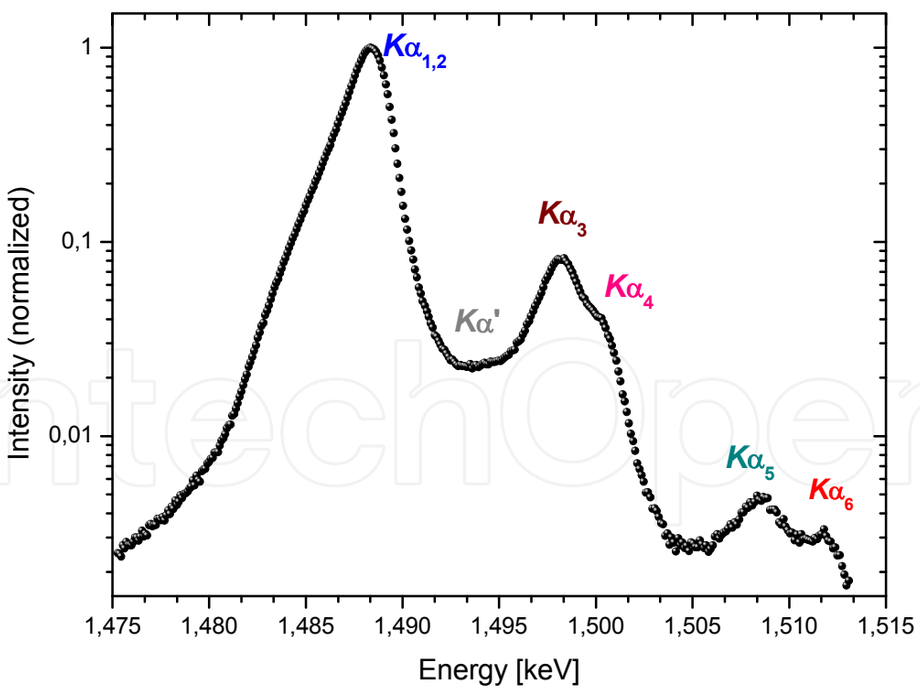

Fig. 5. Al Kα spectrum measured through XRF.

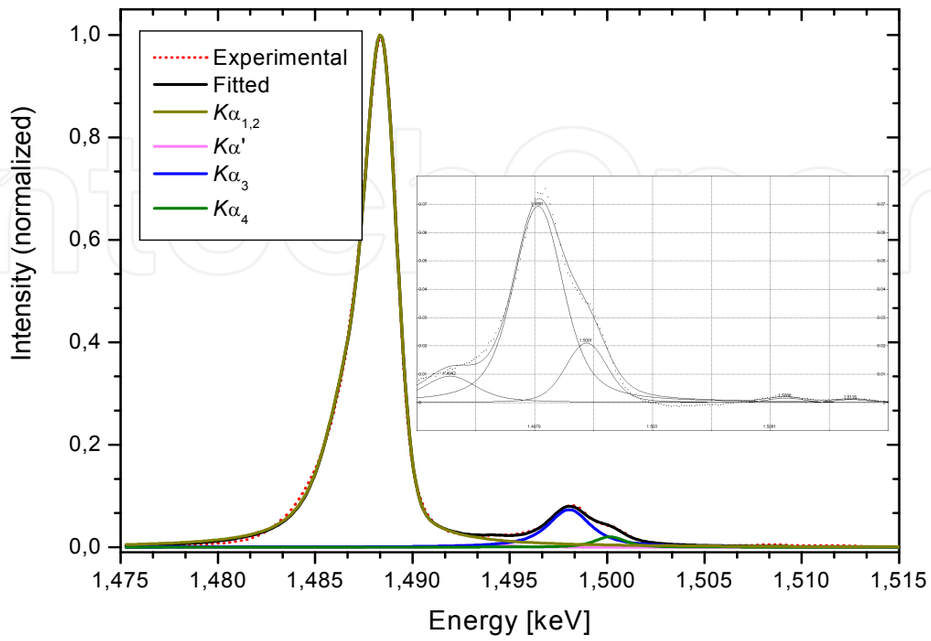

Fig. 6. Al Kα spectrum measured through XRF. Expanded Kα satellites in the top right.

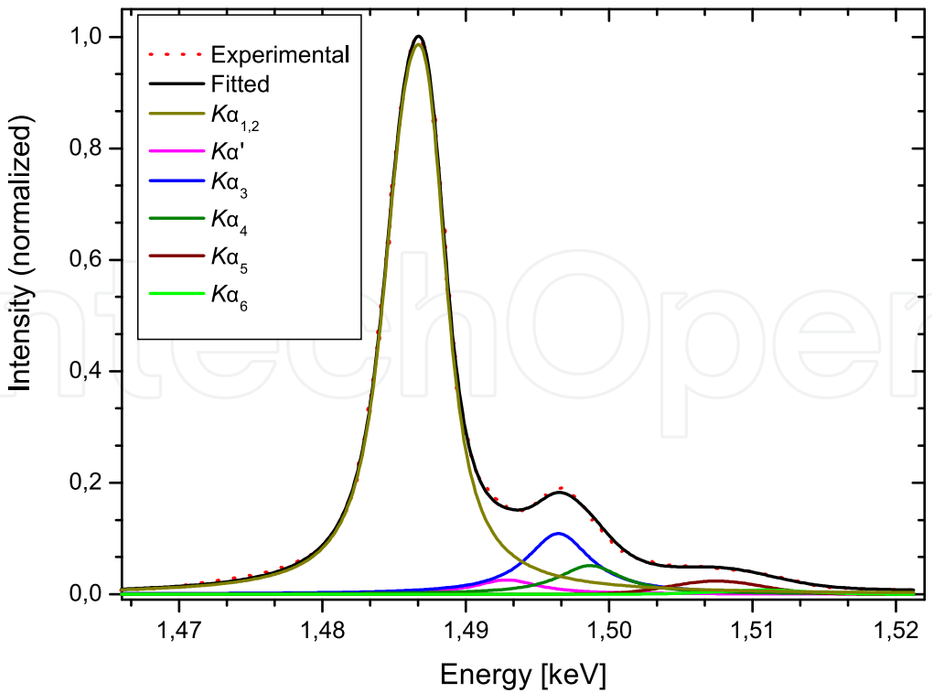

Fig. 7. Al Kα spectrum measured through EPMA. Expanded Kα satellites in the top right.

	XRF (This work)		**XRF** (Other Authors)	
Lines	**Al**	**Al_2O_3**	**Al [*]**	**Al_2O_3 [**]**
$K\alpha_{1,2}$	1486,7	1487,0	-	-
$K\alpha'$	1492,6	1494,0	1492,6	1492,94
$K\alpha_3$	1496,5	1497,2	1496,4	1496,85
$K\alpha_4$	1498,5	1499,2	1498,4	1498,70
$K\alpha_5$	1507,2	1507,8	-	1507,4
$K\alpha_6$	1510,0	1510,4	-	1510,9

Table 1. Energy of Al $K\alpha$ lines in Al and Al_2O_3 (in eV) for single and double ionization, obtained with XRF in this work and by different authors: [*]: (Mauron and Dousse, 2002); [**]: (Wollman et al., 2000).

Table 1 shows that the concordance of our measurements for the energies of the lines Al KL^1 with Mauron and Dousse (Mauron and Dousse, 2002) is remarkable (are equal considering the experimental error), especially if one considers that the latter is a recent work that uses a Von Hamos spectrometer, which was specially designed for this purpose. The same applies to the work of Wollman et al. (Wollman et al., 2000) on the Al_2O_3, whose energy values differ at most in 1 eV for $K\alpha'$ (which is the line with the greatest uncertainty due to its low intensity), and in general the energies of the other lines differ by less than 0.5 eV of ours. In Table 1 we can also see that the energies obtained for the triple vacancy KL^2 lines are very similar to those reported by other authors.

Also in Table 1 we show that the Al $K\alpha$ satellite spectrum changes significantly in the aluminum oxide with regard to the metal: there are shifts in the energy positions of the lines and changes in their relative intensities (see Fig. 8). The shift towards higher energies in the oxide (Al_2O_3) is in agreement with the results found by Liu et al. (Liu, 2004).

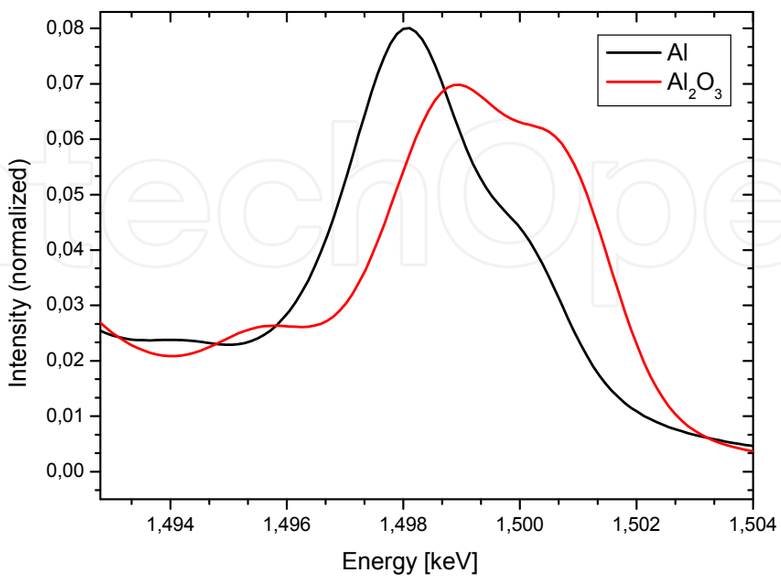

Fig. 8. Satellite spectra of Al and Al_2O_3 measured through XRF.

In Table 2 there are the energies of the lines KL^0 and KL^1 in Al measured by XRF and EPMA in this work, and also those reported in other studies which use different experimental techniques. The major significance of the correlation between the energies measured by us and the ones measured by other authors -whose results are shown comparatively in Table 2-, is the fact that these references relate to works performed with different excitation techniques. Thus, the fact that our results on Al are equal (considering the uncertainties of the measurements) to those of Burkhalter et al. (Burkhalter et al., 1972), obtained with PIXE, reveals the intrinsic nature of the energies of the double-ionization lines, and its independence on the technique used to measure them. Identical energy positions are also observed in our own measurements with XRF and EPMA, confirming this independence on the excitation method.

Line	EPMA$^+$	XRF$^+$	EPMA*	EPMA**	XRF*	PIXE*
$K\alpha_{1,2}$	1486,7	1486,7	1486,7	-	-	1486,6
$K\alpha'$	1492,9	1492,6	1492,3	1492,8	1492,6	1492,8
$K\alpha_3$	1496,5	1496,5	1496,4	1496,5	1496,4	1496,4
$K\alpha_4$	1498,7	1498,5	1498,4	1498,5	1498,4	1498,6

Table 2. Energy in eV of the Al $K\alpha$ lines for single and double ionization, obtained with different techniques and different authors: EPMA$^+$ and XRF$^+$: this work; EPMA*: (Fischer and Baun, 1965); EPMA** and XRF*: (Mauron and Dousse, 2002) ;PIXE*: (Burkhalter et al., 1972).

Fig. 9 and Fig.10 show the double ionization satellite lines measured in Al and in Al_2O_3 with XRF. In these figures, we can see the changes that occur in every satellite line: In the case of $K\alpha'$, it is shifted to higher energy and increases its intensity in the oxide, while the intensities of the lines $K\alpha_4$ and $K\alpha_3$ change from the pure element to an oxide. In particular, it is noted that the intensity ratio between these two lines is $I K\alpha_4 / I K\alpha_3 \cong 0.5$ in the metal, while in the oxide it is $I K\alpha_4 / I K\alpha_3 \cong 1$.

The intensity distribution of the satellite spectrum analyzed, in all spectra measured with both techniques, behaves as follows: $K\alpha'$ is the less intense (10% of $K\alpha_3$), $K\alpha_3$ is the most intense (approximately 10% of $K\alpha_{1,2}$), followed by $K\alpha_4$ (5% of $K\alpha_{1,2}$), except in the aluminum oxide, when the latter two are almost of the same intensity. The ratio of intensities between them ($I K\alpha_4 / I K\alpha_3$) varies in our measurements with EPMA from about 0.5 (in the metal) to 1 in the oxide.

The total intensity of the satellite spectrum with respect to the main one ($I_{satélites}/I K\alpha_{1,2}$, where $I_{satélites} = I K\alpha' + I K\alpha_3 + I K\alpha_4$), is of 10% for XRF and of the order of 20% for EPMA. In Al $K\alpha$ spectrum of oxide, there is a decrease of this intensity with EPMA, and there are no significant changes with XRF. The double vacancy lines are more intense with EPMA, compared to XRF (approximately the double). This confirms the higher probability of double ionization when the sample is excited by charged particles (electrons in our case) than when excited by photons.

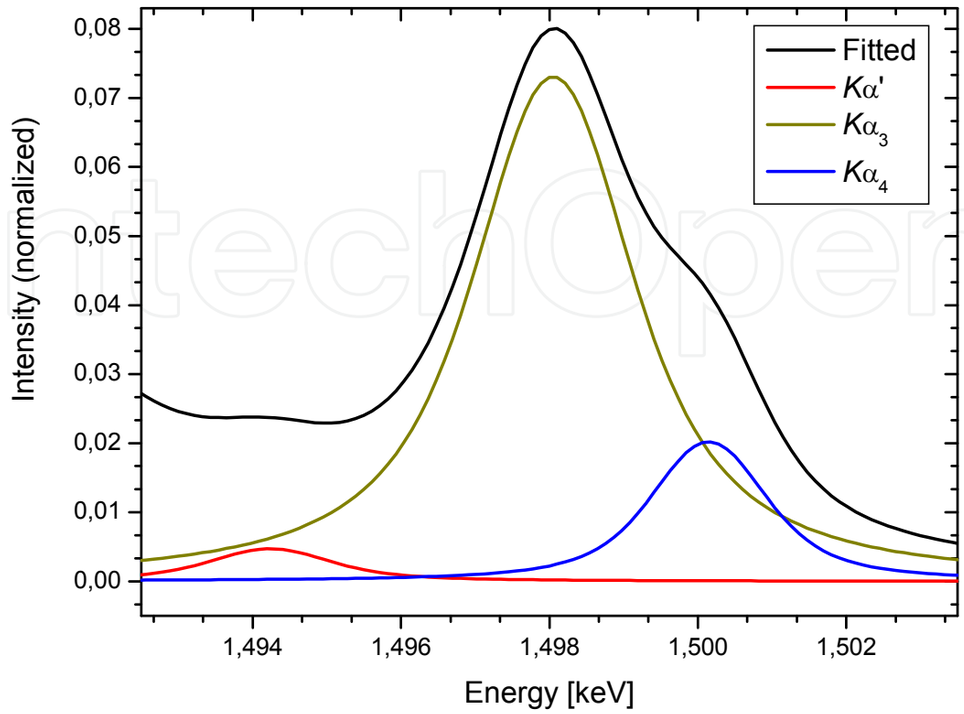

Fig. 9. Satellite lines measured in Al with XRF.

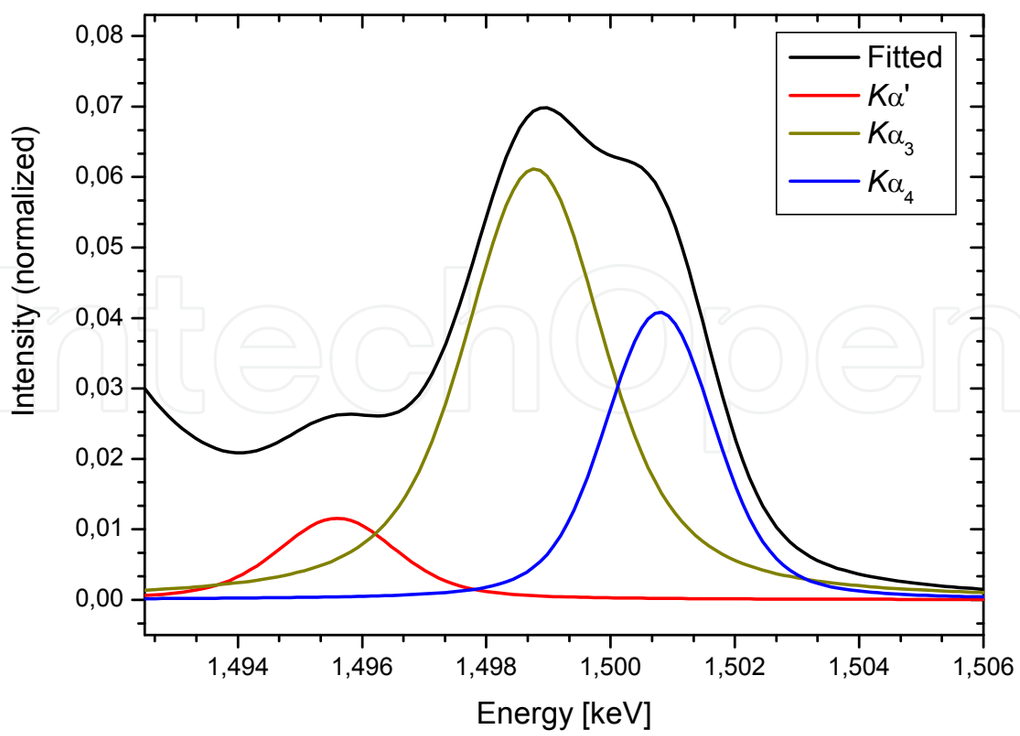

Fig. 10. Satellite lines measured in Al_2O_3 with XRF.

3.2 Satellite lines produced by charge transfer

The effect of charge transfer is important in the compounds formed by the last transition metals. Usually, in these compounds, the 3*d* orbital is the outermost. Then there is the ligand energy level (e.g. in NiF_2, the level of F 2*p*) which is a few eV below of 3*d* of the main atom. So if there was a vacancy in the 1*s* level of the transition element, the 3*d* level is far deeper than the valence bond. This situation is quite unstable, so some electrons from the decay of the F 2*p* level to the level of Ni 3*d* (Kawai, 1993).

3.3 Satellite lines caused by splitting of molecular orbitals

X-rays from transitions from the valence layer to internal orbitals (as the lines *K* and *L*) of elements that are linked to other lighter ones have satellite lines of lower energy than the main peak, with a relative intensity of 5-30% (Urch, 1970). In consequence, these low-energy satellite lines are closely associated with bond formation. The energy separation between these two peaks is a function of the ligand atom (about 20 eV for F, 15 eV for O, 11 eV for N and 8 eV for C) (Esmail et al., 1973). The origin of these lines is just the splitting of molecular orbitals, and can be understood by the simple model of the Molecular Orbital (MO) that was described in the introduction.

Let *p* and *d* orbitals of the valence shell of a central atom (A) in a compound, or a crystalline medium, which is surrounded by x binder atoms (L). The transition *K* ($p \rightarrow 1s$) now displays a structure that reflects a number of molecular orbitals of the form ALx. Light elements, such as C, N, O and F, use their 2*s* and 2*p* orbitals in bond formation. There are therefore two types of molecular orbitals involving electrons A*p*: (A*p*, L2*p*) and (A*p*, L2*s*). Similar arguments can be made for the *L* lines. The energy difference between these two orbitals can be directly measured in appropriate experiments. The presence of these light elements cannot be easily detected using conventional x-ray detectors, which justifies the additional interest in studying this kind of satellite lines.

The occurrence of low energy satellite peaks in the x-ray emission spectrum of the element A, which identify the ligand L, not only shows that L is present in the sample, but also that L is bound to A. The word 'bound' is used in a broad sense, however covalent bonds give more intense satellite peaks. But it is true that ionic bonds are never completely ionic, and even a small percentage of covalent bond is sufficient to generate significant emission peaks.

Among this class of satellite lines, the main one is the *K*β', which is located on the side of lower energies than the $K\beta_{1,3}$, and it originates in the manner described above for those elements of the third period with valence electrons in the 3*p* subshell (Al, Si, P, S and Cl). It is interesting to analyze the *K*β spectrum of the mineral called Topaz, which is an aluminosilicate formed by chains of octahedra of AlO_4F_2. In Topaz, aluminum presents two *K*β' satellite lines, one for each covalent union: Al–O and Al–F (see Fig. 11) (Torres Deluigi et al., 2006). The identification of these satellite lines was done taking into account the energetic separation ΔE between the ionization energies of the *L*2*s* and *L*2*p* orbitals: ΔE ≅ 20, 14, 9 and 5 eV, for F, O, N and C, respectively (Eyring et al., 1944).

In the case of transition metals, the physical origin of the *K*β' line is different. It has been assigned to a strong exchange coupling between unpaired electrons of the valence subshell 3*d* and the unpaired electron of state $3p^5$. The vacancy $3p^{-1}$ is generated by transitions $3p \rightarrow 1s$ that give rise to the line $K\beta_{1,3}$. In contrast, the satellite line *K*β'' of the transition metals have a similar origin to the *K*β' in elements of the third period.

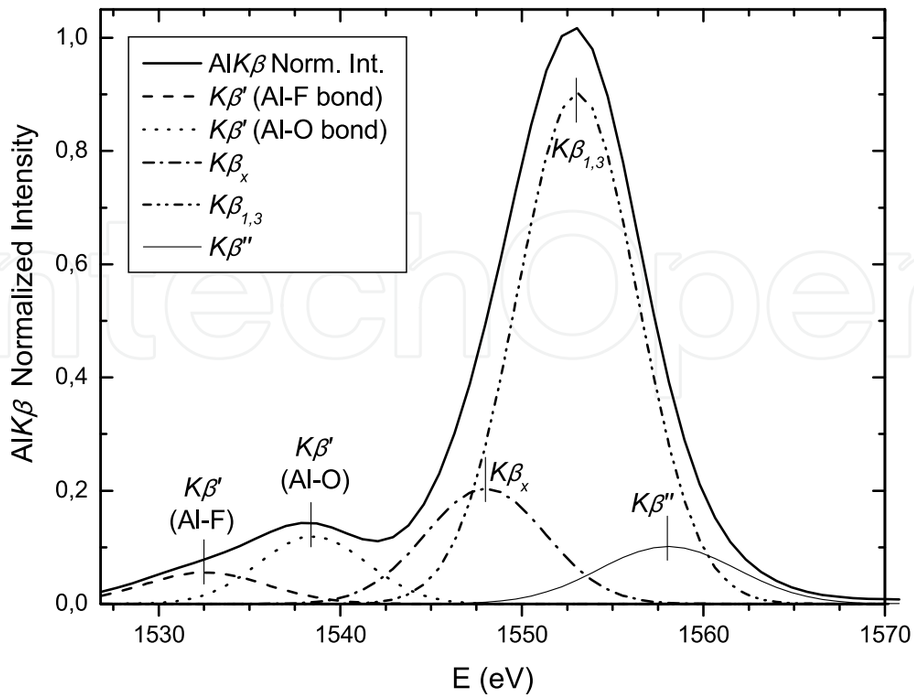

Fig. 11. Al *K*β spectrum of Topaz. The two *K*β′ lines (due to the Al–F and Al–O covalent bonds) and the Al $K\beta_x$, Al $K\beta_{1,3}$ and Al *K*β′′ lines have been deconvoluted with Gaussian functions and its energies are pointed out. The spectrum is normalized to the height at the maximum intensity point. (Torres Deluigi et al., 2006).

Several other theories are available to describe the *K*β′ low energy feature associated with the $K\beta_{1,3}$ emission resulting from transitions involving the partially filled 3*d* shells of transition elements and their oxides (Rémond, 2002). The Radiative Auger Effect (RAE) produces a broad structure at a lower energy than the characteristic diagram line. The RAE process results from a de-excitation of a *K* vacancy, similar to an Auger process with simultaneous emission of a bound electron and an x-ray photon. For transition elements, the low energy structures associated with the $K\beta_{1,3}$ diagram line can be interpreted in terms of *KMM* Radiative Auger Emission (Keski-Rakhonen and Ahopelto, 1980).
According to Salem and Scott (Salem and Scott, 1974), the interaction between the electrons in the incomplete 3*d* shell and the hole in the incomplete 3*p* shell splits both 3*p* and 3*d* levels causing a demultiplication of transitions.
The *K*β′ satellite has also been explained in terms of the plasmon oscillation theory (Tsutsumi et al., 1976). During the x-ray emission process, the transition valence electron excites a plasmon in the valence band. The transition energy of the $K\beta_{1,3}$ line will thus be shared between the plasmon and the emitting photon, which will be deprived of an energy equal to the plasmon energy.

4. Conclusion

High-resolution measurements of the *K* satellite lines in the x-ray emission spectra obtained by XRF and EPMA techniques, provide detailed information on the electronic

structure of the analyzed samples. The profile of the peaks, their energy shifts, the rise of new satellite peaks and the changes in their intensities are all related to chemical and structural properties, such as valence electronic states, the type of bond and the nature of the ligand atom. In particular, the intensity of satellite lines originated by multiple vacancies characterizes the excitation technique used, allowing at the same time to infer information about the internal electronic mechanisms that explain the production of multiple vacancies.

5. Acknowledgments

The authors gratefully acknowledge the involvement of the *Laboratorio de Microscopía Electrónica y Microanálisis* and the *Laboratorio de FRX de Química Analítica* of the *Universidad Nacional de San Luis* (UNSL), Argentina, where measurements were carried out. They also acknowledge the financial support received from the *Secretaría de Ciencia y Tecnología* and the *Proyecto PROICO 2-7502* of the UNSL of the Argentine Republic, which made this publication possible.

6. References

Aberg, T. (1927). Theory of multiple ionization processes, *Proc. Int. Conf. Inner Shell Ionization Phenomena*, USAEC Conf. 720404 USA EC, Atlanta, GA, 1927, pp. 1509-1542

Adachi, H., Tsukada, M. & Satoko, C. (1978). Discrete Variational Xα Cluster Calculations. I. Application to Metal Clusters. *J. Phys. Soc. Jpn.*, Vol. 45, N°3, (September 1978), pp. (875-883), ISSN 0031-9015

Burkhalter, P. G., Knudson, A. R., Nagel, D. J. & Dunning, K. L. (1972). Chemical Effects on Ion-Excited Aluminum K X-Ray Spectra. *Phys. Rev. A,* Vol. 6, (December 1972), pp. (2093-2101), ISSN 1050-2947

Cotton, F. A. & Wilkinson, G. (2008). *Química Inorgánica Aplicada = Advanced inorganic chemistry* (4th Ed.), Limusa, ISBN: 978-968-18-1795-4 , Mexico

Endo, H., Uda, M. & Maeda, K. (1980). Influence of the chemical bond on the intensities of F Kα x-ray satellites produced by electron and photon impacts. *Phys. Rev.* A, Vol. 22, (October 1980), pp. (1436-1440), ISSN 1050-2947

Esmail, E. I., Nicholls, C. J. & Urch, D. S. (1973). The detection of light elements by X-ray emission spectroscopy with use of low-energy satellite peaks. *Analyst*, Vol. 98, (October 1973), pp. (725-731), ISSN 0003-2654

Eyring, H., Walter, J. & Kimball, G. E. (1944). *Quantum Chemistry*, John Wiley & Sons Inc., New York

Fischer, D. W. & Baun, W. L. (1965). Diagram and Nondiagram Lines in K Spectra of Aluminum and Oxygen from Metallic and Anodized Aluminum. *J. Appl. Phys.*, Vol. 36, (February 1965), pp. (534-537), ISSN 0021-8979

Kawai, J. (1993). Chemical effects in the satellites of X-ray emission spectra. *Nucl. Instr. and Meth. in Phys. Res. B*, Vol. 75, (April 1993), pp. (3- 8), ISSN 0168-583X

Keski-Rakhonen, O. & Ahopelto, J. (1980). The K-M2 radiative Auger effect in transition metals. *J. Phys. C: Solid State Phys.*, Vol. 13, N° 4, (February 1980), pp. (471-482), ISSN 0022-3719.

Knudson, A. R., Nagel, D. J., Burkhalter, P. G. & Dunning, K. L. (1971). Aluminum X-Ray Satellite Enhancement by Ion-Impact Excitation. *Phys. Rev. Lett.,* Vol. 26, (May 1971), pp. (1149-1152), ISSN 0031-9007

Lui, Z., Sugata, S., Yuge, K., Nagasono, M., Tanaka, K. & Kawai, J. (2004). Correlation between chemical shift of Si Kα lines and the effective charge on the Si atom and its application in the Fe-Si binary system. *Phys. Rev. B,* Vol. 69, (January 2004), pp. (035106-035110), ISSN 1098-0121

Mauron, O. & Dousse, J.-Cl. (2002). Double KL ionization in Al, Ca, and Co targets bombarded by low-energy electrons. *Phys. Rev. A,* Vol. 66, (October 2002), pp. (042713-042726), ISSN 1050-2947

Mogi, M., Ota, A., Ebihara, S., Tachibana, M. & Uda, M. (1993). Intensity analysis of S Kß emission spectra of Na2SO3 by the use of DV-Xα MO method. *Nucl. Instr. and Meth. in Phys. Res. B*, Vol. 75, (April 1993), pp. (20-23), ISSN 0168-583X

Mukoyama, T., Taniguchi, K. & Adachi, H. (1986). Chemical effect on Kβ:Kα x-ray intensity ratios. *Phys. Rev. B*, Vol. 34, N° 6, (September 1986), pp. (3710-3716), ISSN 1098-0121

Oura, M., Mukoyama, T., Taguchi, M., Takeuchi, T., Haruna, T. & Shin, S. (2003). Resonant Double Excitation Observed in the Near-Threshold Evolution of the Photoexcited F Kα Satellite Intensity in NaF. *Phys. Rev. Lett.,* Vol. 90, (May 2003), pp. (173002-173005), ISSN 0031-9007

Parratt, L. G. (1936). K satellites. *Phys. Rev.,* Vol. 50, (July 1936), pp. (1-15)

Parratt, L. G. (1959). Electronic band structure of solids by x-ray spectroscopy. *Rev. Mod. Phys.*, Vol. 31, N°. 3, (July 1959), pp. (616-645), ISSN 0034-6861

Randall, C. A. & Parratt, L. G. (1940). Lα satellite lines for elements Mo(42) to Ba(56). *Phys. Rev. A*, Vol. 57, (May 1940), pp. (786-791), ISSN 1050-2947

Rémond, G., Myklebust, R., Fialin, M., Nockolds, C., Phillips, M. & Roques-Carmes, C., *J.* (2002). Decomposition of wavelength dispersive X-ray spectra. *J. Res. Natl. Inst. Stand. Technol.*, Vol. 107, N° 6, (November–December 2002), pp. (509–529), ISSN 0160-1741

Salem, S. I. & Scott, B. L. (1974). Splitting of the 4d 3/2 and 4d 5/2 levels in rare-earth elements and their oxides. *Phys. Rev. A*, Vol. 9, (February 1974), pp. (690-696), ISSN 1050-2947

Torres Deluigi, M., Strasser, E. N., Vasconcellos, M. A. Z. & Riveros, J. A. (2006). Study of the structural characteristics of a group of natural silicates by means of their Kβ emission spectra. *Chem. Phys.,* Vol. 323, (April 2006), pp. (173-178), ISSN 0301-0104

Tsutsumi, K., Nakamori, H. & Ichikawa, K. (1976). X-ray MnKβ emission spectra of manganese oxides and manganates. *Phys. Rev. B*, Vol. 13, (January 1976), pp. (929-933), ISSN 1098-0.121

Uda, E., Kawai, J. & Uda, M. (1993). Calculation of sulfur Kβ X-ray spectra. *Nucl. Instr. and Meth. in Phys. Res. B*, Vol. 75, (April 1993), pp. (24-27), ISSN 0168-583X

Uda, M., Endo, H., Maeda, K., Awaya, Y., Kobayashi, M., Sasa, Y., Kumagai, H., Tonuma, T. (1979). Bonding Effect on F Kα Satellite Structure Produced by 84-MeV N4+. *Phys. Rev. Lett.,* Vol. 42, (May 1979), pp. (1257-1260), ISSN 0031-9007

Urch, D. S. (1970). The origin and intensities of low energy satellite lines in X-ray emission spectra: a molecular orbital interpretation. *J. Phys. C: Solid State Phys.*, Vol. 3, (June 1970), pp. (1275-1291), ISSN 1361-6455

Urch, D. S. (1979). X-ray Emission Spectroscopy, In: *Electron Spectroscopy: Theory, Techniques and Applications, Vol. 3,* C. R. Brundle, A. D. Baker, pp. (1-39), Academic Press, Londres

Urch, D. S. (1985). X-ray Spectroscopy and Chemical Bonding in Minerals, In: *Chemical Bonding and Spectroscopy in Mineral Chemistry,* F. J. Berry, D. J. Vaughan, pp. (31-61), Chapman & Hall, Londres

Wollman, D. A., Nam, S. W., Newbury, D. E., Hilton, G. C., Irwin, K. D., Bergren, N. F., Deiker, S., Rudman, D. A. & Martinis, J. M. (2000). Superconducting transition-edge-microcalorimeter X-ray spectrometer with 2 eV energy resolution at 1.5 keV. *Nucl. Instr. and Meth. in Phys. Res. A,* Vol. 444, (April 2000), pp. (145-150), ISSN 0168-9002

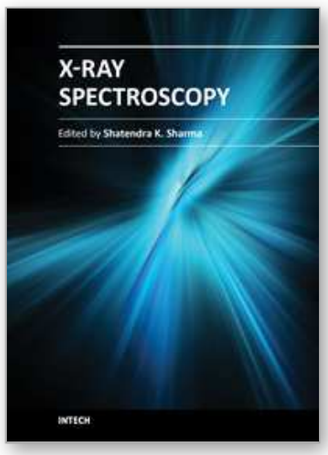

X-Ray Spectroscopy

Edited by Dr. Shatendra K Sharma

ISBN 978-953-307-967-7

Hard cover, 280 pages

Publisher InTech

Published online 01, February, 2012

Published in print edition February, 2012

The x-ray is the only invention that became a regular diagnostic tool in hospitals within a week of its first observation by Roentgen in 1895. Even today, x-rays are a great characterization tool at the hands of scientists working in almost every field, such as medicine, physics, material science, space science, chemistry, archeology, and metallurgy. With vast existing applications of x-rays, it is even more surprising that every day people are finding new applications of x-rays or refining the existing techniques. This book consists of selected chapters on the recent applications of x-ray spectroscopy that are of great interest to the scientists and engineers working in the fields of material science, physics, chemistry, astrophysics, astrochemistry, instrumentation, and techniques of x-ray based characterization. The chapters have been grouped into two major sections based upon the techniques and applications. The book covers some basic principles of satellite x-rays as characterization tools for chemical properties and the physics of detectors and x-ray spectrometer. The techniques like EDXRF, WDXRF, EPMA, satellites, micro-beam analysis, particle induced XRF, and matrix effects are discussed. The characterization of thin films and ceramic materials using x-rays is also covered.

InTech Europe
University Campus STeP Ri
Slavka Krautzeka 83/A
51000 Rijeka, Croatia
Phone: +385 (51) 770 447
Fax: +385 (51) 686 166
www.intechopen.com

InTech China
Unit 405, Office Block, Hotel Equatorial Shanghai
No.65, Yan An Road (West), Shanghai, 200040, China
中国上海市延安西路65号上海国际贵都大饭店办公楼405单元
Phone: +86-21-62489820
Fax: +86-21-62489821

IntechOpen